

Electronic Supplementary Information

Ultrafast-Charging Solid-State Al-ion Batteries with an Ultralong Cycle Life

Xuejing Shen,^a Sun Tao,^{*a} Zhanjun Wu^{*a} and Li Tan^{*b}

^a School of Aeronautics and Astronautics, State Key Laboratory of Structural Analysis for Industrial Equipment, Dalian University of Technology, Dalian 116024, China.

^b Department of Mechanical & Materials Engineering, University of Nebraska, Lincoln, NE 68588, USA.

*E-mail: tsun@dlut.edu.cn; wuzhj@dlut.edu.cn; ltan4@unl.edu

Material and methods

Chemicals and materials

They were purchased from the following vendors unless otherwise specified: acrylamide (AAM, >99%), N,N-methylenebisacrylamide (MBAA, >99%), poly (methyl methacrylate) (PMMA, Mw 996000) from Sigma-Aldrich; anhydrous dichloromethane (DCM, >99%), anhydrous aluminum chloride (AlCl_3 , 99.985%) from Alfa Aesar; 1-ethyl-3-methylimidazolium chloride (EMI-Cl, >98.0%), 2,2'-azobisisobutyronitrile (AIBN, >98%) from TCI; anisole (99%) from Aladdin; nickel foam (1.6 mm in thickness, 0.1 mm in diameter, purity >99.9%) from Alantum Advanced Technology Materials (Dalian) Co., Ltd.; aluminum foil (50 μm in thickness, 99.999%) from Beijing Trillion Metals Co., Ltd.; molybdenum foil (30 μm in thickness, 99.95%) from Baoji Teska Rare Metals Co., Ltd.; colloidal silver (60% silver content) from Electron Microscopy Sciences; Above materials and chemicals were all used as received without further purifications.

Preparation of ionic liquid

The ionic liquid was made in an argon-filled glovebox by mixing 1-ethyl-3-methylimidazolium chloride (EMI-Cl) (solid) and anhydrous powers of aluminum chloride (AlCl_3) ($\text{AlCl}_3/\text{EMI-Cl}$ mole ratio = 1.5). The resulting light-yellow, transparent liquid was stirred at room temperature for 12 h and settled for using.

Preparation of gel polymer electrolyte (GPE)

GPE was prepared by four steps: (1) adding acrylamide (AAM/ AlCl_3 mole ratio = 1) in the suspension of anhydrous aluminum chloride (14 wt% AlCl_3 in DCM); (2) adding desired amount of ionic liquid (80~95 wt%); (3) adding the cross-linker MBAA (3 wt% of monomer); (4) after adding AIBN initiator (1 wt% of monomer), pouring the solution into a Teflon ($20 \times 20 \times 2 \text{ mm}^3$) mold for 24 h settling. All the procedures were carried out in an argon-filled glovebox.

Preparation of 3D graphene cathode

Three-dimensional (3D) graphene was grown by chemical vapor deposition (CVD) inside the horizontal tube furnace (HF-Kejing, OTF-1200X-80SL). At first, the Ni foam was cleaved into a desired shape ($35 \times 60 \text{ mm}^2$) and then thoroughly rinsed with the following solvents: toluene, acetone, copious de-ionized (DI) water, and anhydrous ethanol. After drying, the Ni foam was loaded into the quartz tube and pumped to a pressure below 1 Pa. Subsequently, a constant flow

of H₂ (119 standard cubic centimeters per minute or s.c.c.m) was introduced into the chamber, while the tube was heated to 1000 °C. After keeping 20 mins, the heating was elevated to 1100 °C and a constant flow of methane (80 s.c.c.m) was introduced to trigger the growth of 3D graphene over Ni foam. The entire growth process lasted 60 minutes, after which the furnace was cooled down to near room temperature over half an hour (see Figure S6 for control parameters). Resulting 3D Ni@graphene foam was then dip-coated with a thin layer of PMMA (4 wt% PMMA solution in anisole) and baked at 95 °C for 4 h. The Ni@3D graphene@PMMA foam was then cut into pieces with desired dimensions (15 × 17 mm²; 5 × 8 mm²). Afterwards, these pieces were placed in a HCl bath (3.0 M, 70 °C) for 4 h to completely dissolve the Ni layer and later soaked in DI water (5 times) to remove the inorganic residue. Next, the 3D graphene@PMMA sample was soaked in acetone (6 times) at 50 °C for 1 h, then being placed in anhydrous ethanol and later transferred to a supercritical CO₂ dryer (Tousimis, Samdri-795) where its small chamber was preloaded with 20 mL anhydrous ethanol. Liquid CO₂ was pumped into the chamber to keep the pressure at 850 psi. The temperature was kept below 10 °C and purged for 3-5 minutes. A heater was then used to raise the temperature and pressure in the chamber respectively to 31 °C and 1250 psi (for 4 minutes). Finally, the pressure in the small chamber was released, and the 3D graphene was recovered.

Solid-state battery construction

Solid-state batteries were also assembled in the argon-filled glovebox. These cells used 3D graphene as the cathode (density of 0.25 mg cm⁻²), Al foil as the anode (thickness of 50 μm), and a GPE membrane as the electrolyte (solid-state). For the cathode, Mo foils were used as the current collector, with colloidal silver as the adhesive and epoxy as the fixing layer. The cathode and GPE were fixed together by the following step: putting 3D graphene with a certain size was putted into Teflon mode; adding GPE precursors until graphene was completely submerged; standing for 24h for the polymerization of GPE.

Electrochemical measurements

Multi-cycled test was carried out on a battery testing system (LANHE, CT3001A). For the fast galvanostatic charge/discharge tests, since the number of points collected has a great impact on quantified device performances, these tests were performed on an electrochemical analyzer (CH Instruments, CHI660E; minimum data interval: 0.1 ms). Specific capacity data reported here are all based on the mass of graphene only. Aluminum plating and stripping, cyclic voltammetry (CV) (0-2.6 V, 10 mV s⁻¹) and electrochemical impedance spectroscopy (EIS) measurements

(two-electrode mode, 100 kHz ~ 0.1 Hz, 5 mV) were also operated on CHI660E. The battery used 3D graphene as the working electrode and Al as the counter and reference electrode.

Structure and morphology characterization

An optical microscope (PUDA, MM-8C) with a digital camera (ToupCamTM, TP614000A) was used to record the images of aluminum plating and stripping. For top-view observations, two pieces of Al foil were placed horizontally on a glass slide. Then the foils were covered with a GPE membrane, followed by a cover glass on the top. For side-view observations, the GPE membrane was bridged between two Al foils that was laid side by side. After adding a cover glass on the top, a slight pressure was applied to ensure a good contact. The cells were finally sealed with polyimide tape and then taken outside the glovebox for testing. The structure of 3D graphene was characterized by field emission scanning electron microscopy (FE-SEM; JSM-7610F Plus). The uniaxial tension operation of the GPE was performed on a precise micro-loading device, which is equipped with a screw displacement loading system with precision up to 10 μm , and installed with a micro-force measuring system with precision up to 1 mN.

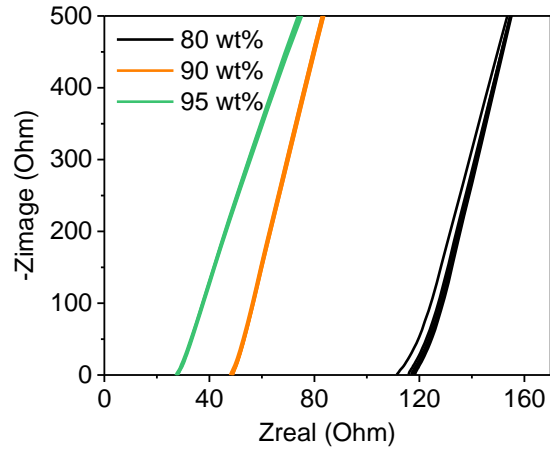


Fig. S1. Electrochemical impedance spectroscopy (EIS) from GPE membranes with 80~95 wt% content of ionic liquid. The corresponding ionic conductivity was determined by

$$\sigma = R_b^{-1} S^{-1} d$$

Where σ is ionic conductivity, R_b the intercept at the real axis in the Nyquist plot, S is the geometric area of the electrolyte-electrode interface, and d is the film thickness ($d = 2$ mm). Five measurements were performed for each sample.

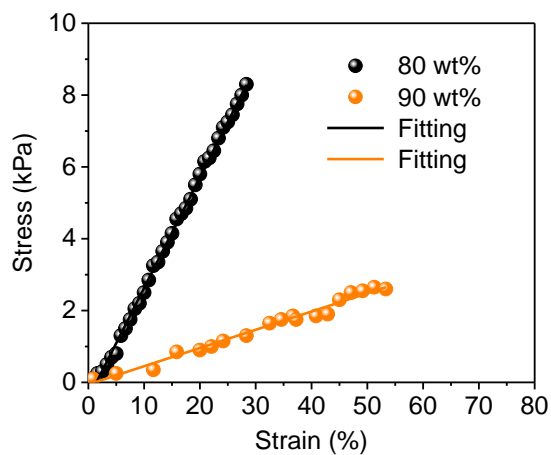


Fig. S2. Topical stress-strain curves of the gel polymer electrolyte (GPE) membrane. A GPE membrane with 80 wt% ionic liquid exhibited greater strength and less elongation than that with 90 wt% ionic liquid. Young's modulus obtained from fitting curves, i.e., $E_{80 \text{ wt}\%} = 30.8 \text{ kPa}$, $E_{90 \text{ wt}\%} = 5.1 \text{ kPa}$.

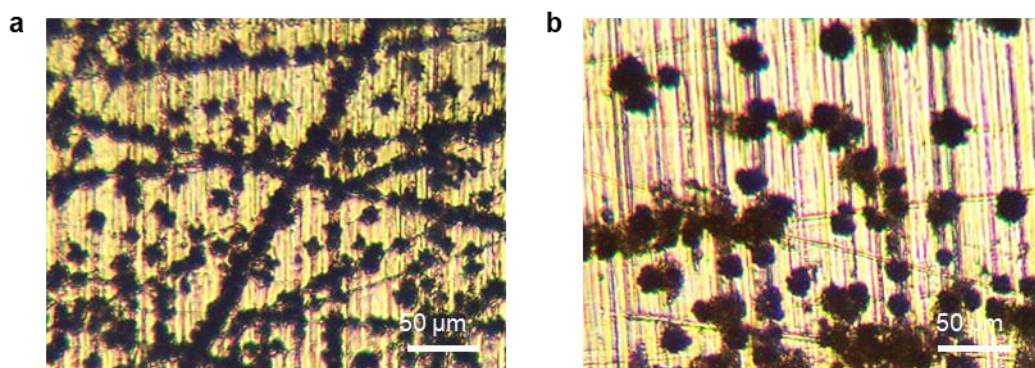


Fig. S3. Different growth patterns of newly grown aluminum on rigid and soft GPE membranes. The optical microscope (OM) image of Al foil under a rigid (**a**) or soft (**b**) GPE membrane after 100 s plating at current density of 1.5 mA cm^{-2} .

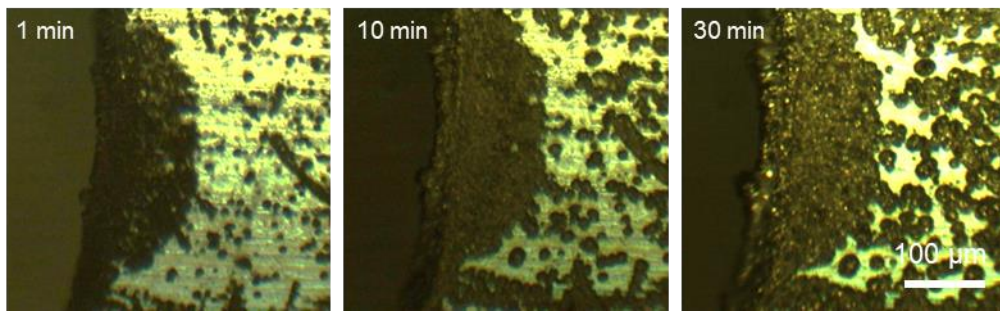


Fig. S4. The plating process of Al metal using a liquid electrolyte. OM images after Al plating (1 ~ 30 min) under current density of 1.5 mA cm^{-2} .

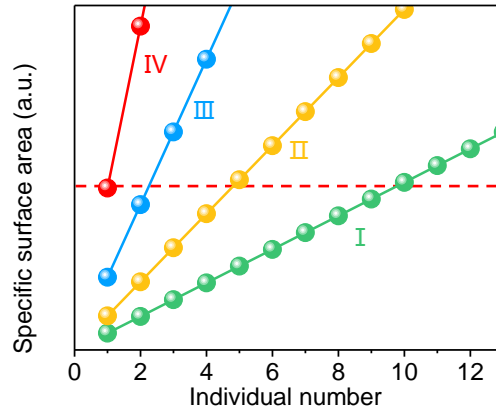


Fig. S5. The relationship between the number of fractal dendrites and the specific surface area. Higher degree of fractal level in dendrites requests less individual number in gaining the same amount of surface areas.

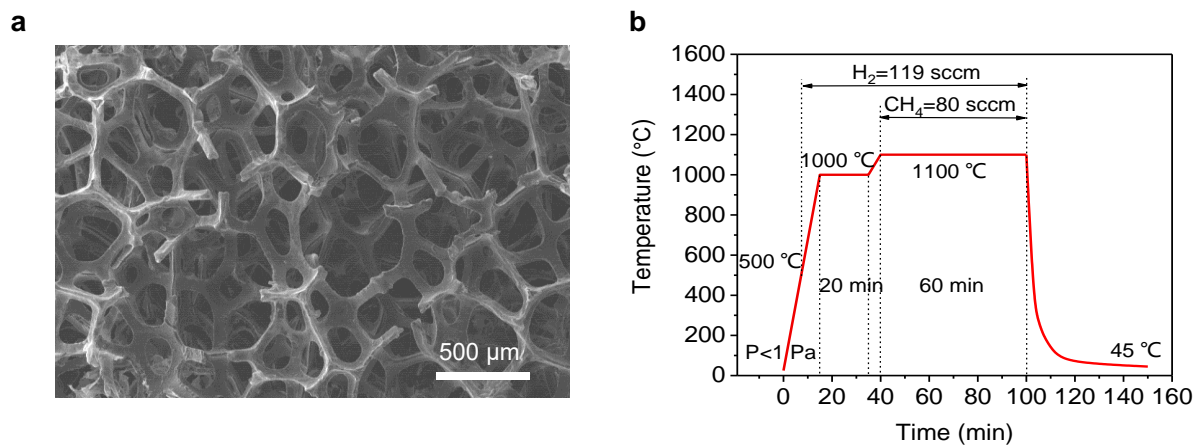


Fig. S6. Network structure and growth parameters of 3D graphene. (a) SEM images of 3D graphene that dried with supercritical CO₂. (b) Control parameters of chemical vapor deposition (CVD) used for the growth of graphene.

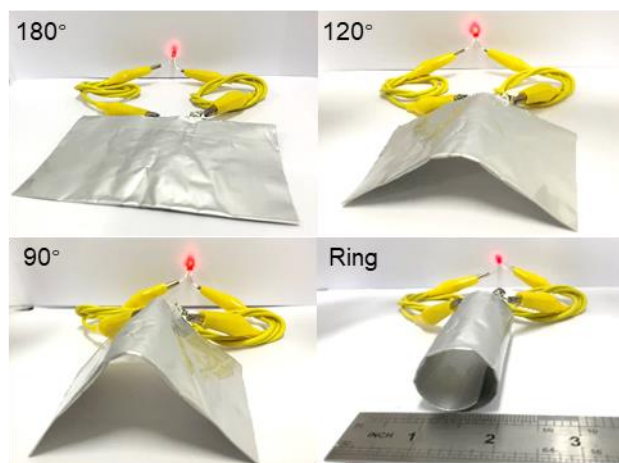


Fig. S7. The battery powers an LED bulb under different states of bending.

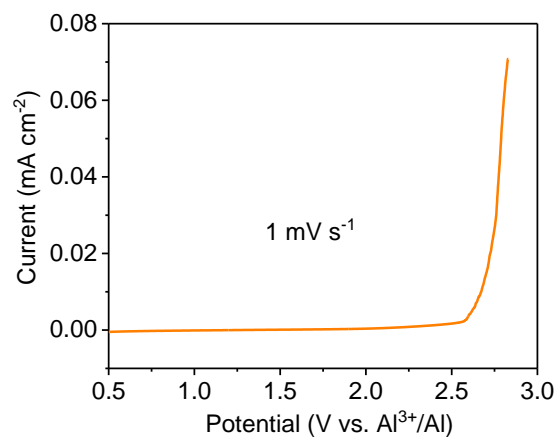


Fig. S8. Linear-sweep voltammetry (LSV) curve of the GPE membrane. No pronounced peak or noticeable oxidation current was found up to 2.7 V (versus Al/Al³⁺), which implies that the GPE is proved to be stable within the operating voltage window.

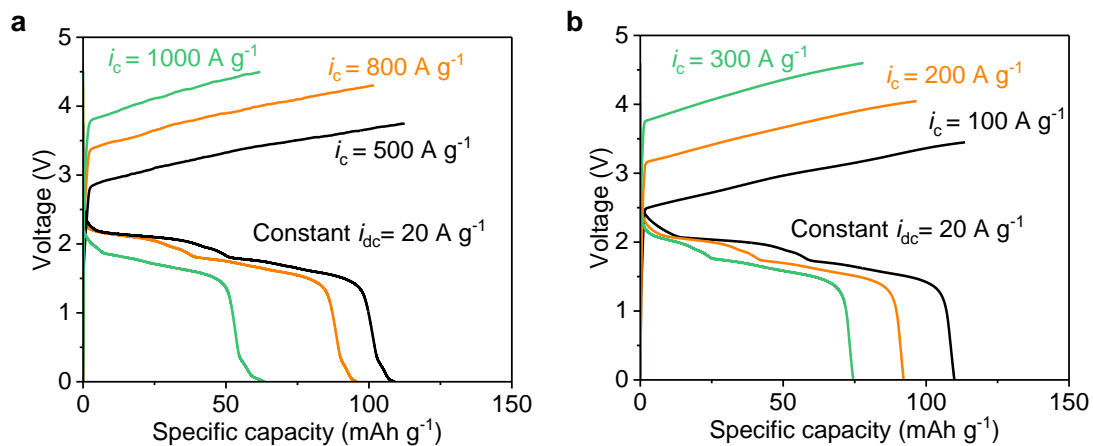


Fig. S9. Ultrafast charge and moderate discharge curves of the battery using a soft (a) or rigid (b) GPE. Moderate discharging ($i_{dc} = 20 \text{ A g}^{-1}$) after a fast charging ($i_c = 100 \sim 1000 \text{ A g}^{-1}$) leads to upward shifting in discharging voltage plateaus and better release in specific capacities.

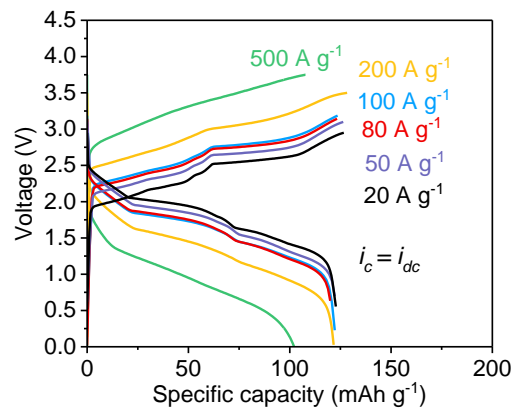


Fig. S10. Typical galvanostatic charge and discharge curves of the device with a soft GPE at different current densities.

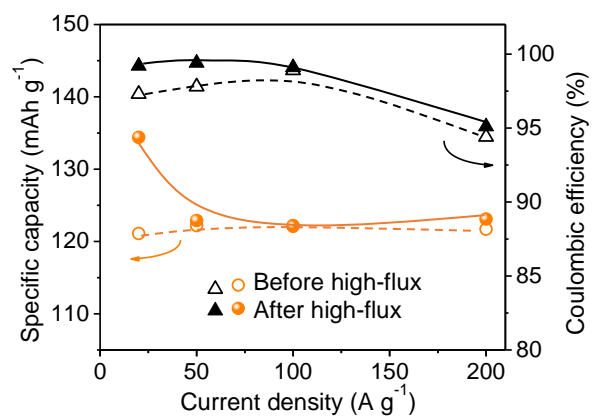


Fig. S11. Trajectory of device performance at different current densities ($i_c = i_{dc} = 20 \sim 200$ A g⁻¹). Higher capacity and better efficiency obtained after a high-flux treatment.

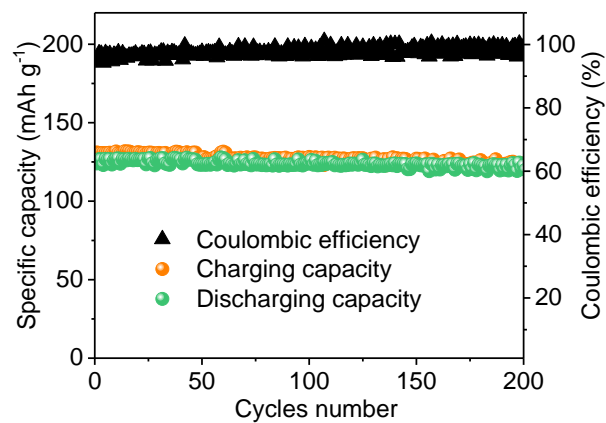


Fig. S12. Initial cycles of a device at current density of 5 A g^{-1} . The device was activated to achieve high Coulombic efficiency.

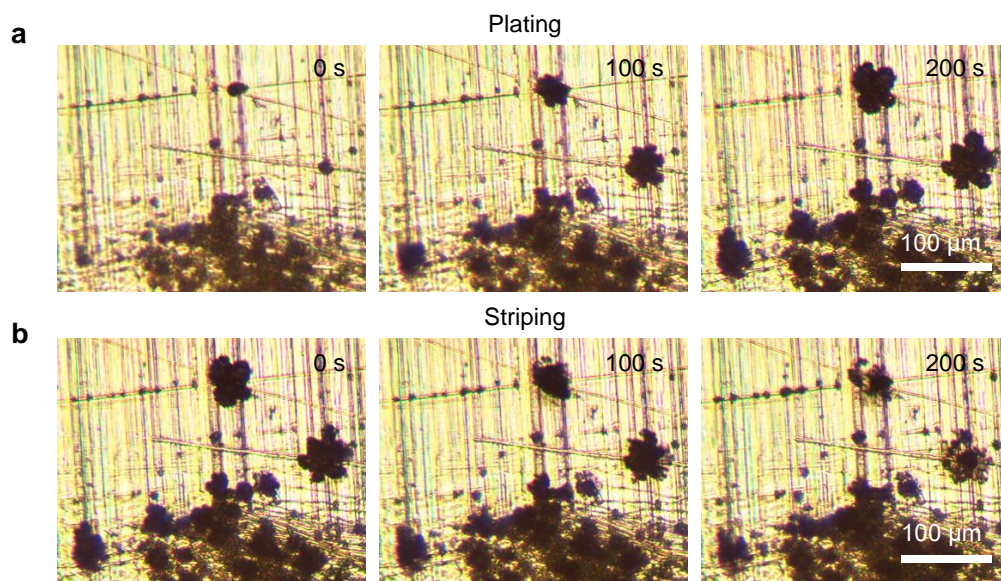


Fig. S13. The plating and stripping process of Al metal under a GPE membrane. OM images of Al plating (a) and stripping (b) under current density of 1.5 mA cm^{-2} .

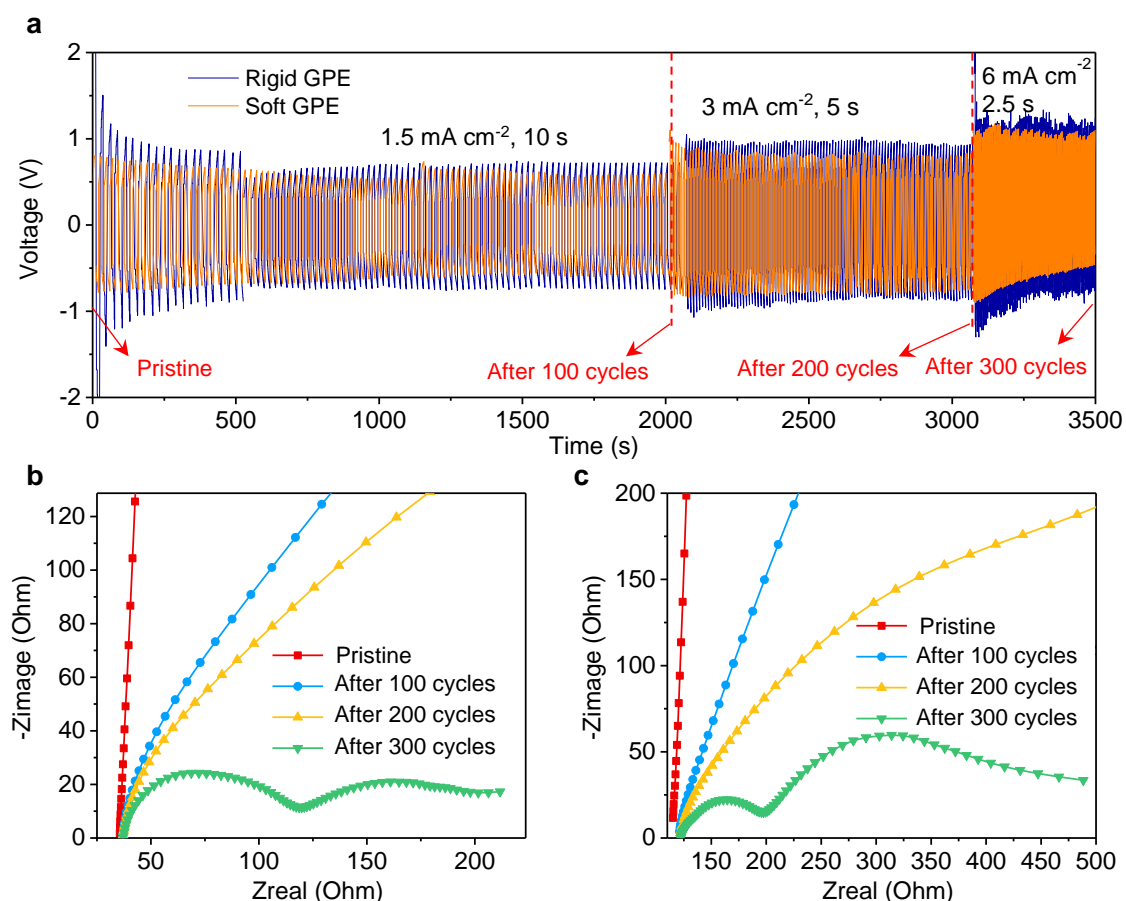


Fig. S14. EIS results of symmetric Al/GPE/Al cells before and after cycles. (a) The aluminum deposition/stripping of the cell using a rigid or a soft GPE membrane at different current densities. (b-c) Nyquist plots of the Al/GPE/Al cell with a soft (b) or a rigid (c) GPE before and after cycles. The EIS in frequency range of 100 kHz ~ 0.1 Hz with an amplitude of 5 mV was conducted. In comparison, the Al/GPE/Al cell with a soft GPE membrane presented lower polarization voltages and smaller charge transfer resistance than the cell with a rigid GPE. In both cases, their resistances decreased after the cycling process and reduced further as the increase of current density.

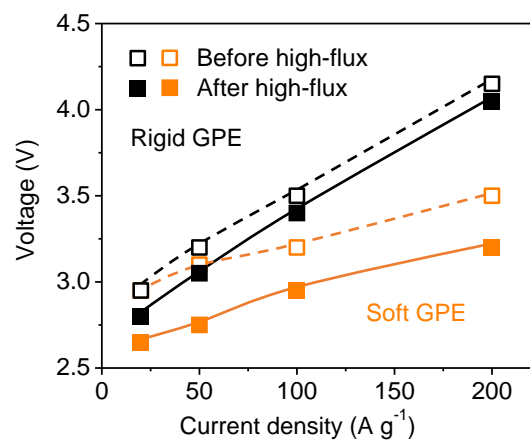


Fig. S15. Effect of high-flux treatment on battery with a soft or a rigid GPE. The efficacy in lowering the saturation voltage with a rigid GPE was less prominent.

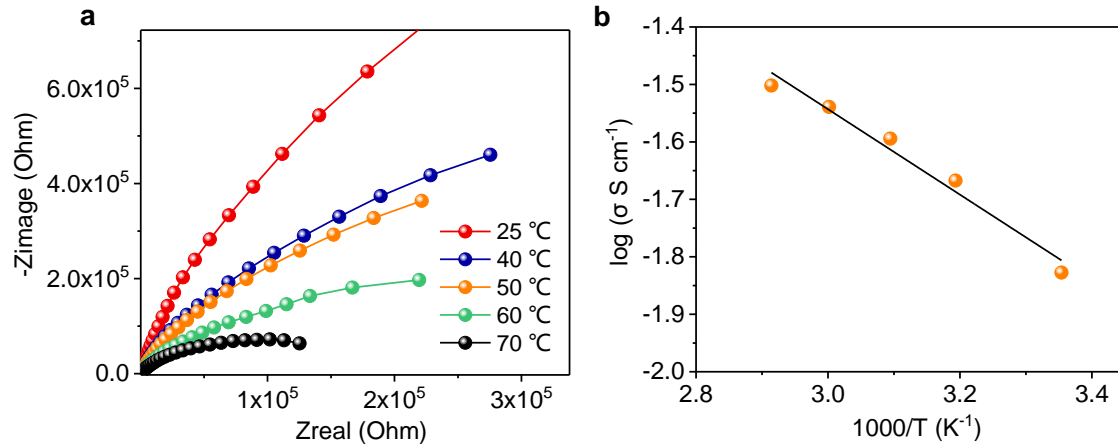


Fig. S16. The measurement of activation energy of GPE. (a) The Nyquist plot of the Mo/GPE/Mo cell in the frequency range from 100 kHz to 0.1 Hz, with an amplitude of 5 mV in the temperature range of 25 ~ 70 °C. (b) Arrhenius conductivity plot for the ionic conductivity.

The activation energy of GPE (90 wt% ionic liquid) was calculated by the Arrhenius equation:

$$\sigma = \sigma_0 \exp\left(-\frac{E_a}{kT}\right)$$

where σ_0 is the pre-exponential factor, E_a is the activation energy, k is the Boltzmann constant, and T is the temperature. By calculating the slopes in Fig. S10b, the activation energy E_a in GPE membranes here was evaluated to be 0.064 eV.

Table S1. Energy (eV) calculated by DFT

Species	Vacuum	Solvation
Al ³⁺	-6542	-6568
AlCl ₄ ⁻	-56702	-56704
Al ₂ Cl ₇ ⁻	-100876	-100878
Al ₃ Cl ₁₀ ⁻	-145050	-145051
ΔG ₁	48.58	15.58
ΔG ₂	48.25	15.42

All compounds were fully optimized by employing density functional theory (DFT) with B3LYP functional at the 6-311+G(d) basis set levels. Structure optimizations were calculated in both vacuum and solvent environment (to take account the solvation effect). The solvent effect (in water) was taken into account using the polarized continuum model (PCM) for all calculations. There are no imaginary frequencies for all the structures of optimization, which indicates that all the optimized structures are the minima on the potential energy surfaces and are stable structures.

As dendrites grown by high-flux operations have produced more surface areas, there was a lower local current density at the dendrite-grown interface compared with that at the dendrite-absent surface (before high-flux). Namely, under the same input current, the local current density of the anode-GPE interface before and after high-flux treatment were large and relatively small, respectively. In order to meet the energy threshold of reactions at high-rate operation, the negatively charged complexes (AlCl₄⁻, Al₂Cl₇⁻) could have formed triple-complex (Al₃Cl₁₀⁻) or polymeric complexes. Thus, Equation 1a and 2a are therefore describing these two states:



In order to compare the reduction potential, we used positively charged Al³⁺ to replace the electrons as following:



Higher ΔG₁ (Equation 1b) was always obtained than ΔG₂ (Equation 2b), be it in vacuum or in solvent, as shown in Table S1. According to the Nernst equation, the reduction potential of

Equation 1a will be greater than that of Equation 2a. This matches with our experimental observations, in which high-flux treated device (Equation 2a) had a larger potential difference than that before the treatment (Equation 1a).

Table S2. Electrochemical properties of our work and state-of-the-arts

Solid-state electrolyte	Content of ionic liquid (wt %)	Electrodes	Specific capacity (mAh g ⁻¹)	Highest charging current density (A g ⁻¹)	Cycle number (capacity retention)	Ref.
Acrylamide + MBAA + EMIC-AlCl ₃	90 (free-standing)	3D graphene + activated Al	134 (@ 20 A g ⁻¹)	1000 (63.4 mAh g ⁻¹)	20000 (85.2%)	This work
Acrylamide + EMIC-AlCl ₃	80	Graphite + Al	120 (@ 0.06 A g ⁻¹)	0.3 (84 mAh g ⁻¹)	100 (88.6%)	[30]
Acrylamide + Et ₃ NHCl-AlCl ₃	80	Graphite + Al	120 (@ 0.5 A g ⁻¹)	2 (91 mAh g ⁻¹)	800 (97.8%)	[31]
Polyamide + Et ₃ NHCl-AlCl ₃	66.7	Graphite + Al	94.6 (@ 0.2 A g ⁻¹)	1 (67.3 mAh g ⁻¹)	2000 (~95%)	[33]
Ethyl acrylate + MBAA + EMIC-AlCl ₃	50 (free-standing)	Graphite + Al	93 (@ 0.1 A g ⁻¹)	0.5 (63 mAh g ⁻¹)	500 (95%)	[34]
MOF + EMIC-AlCl ₃	65 (free-standing)	Graphite + Al	85 (@ 0.02 A g ⁻¹)	0.2 (53 mAh g ⁻¹)	2000 (88.6%)	[35]